Available online at www.sciencedirect.com

ScienceDirect

Physics Procedia 56 (2014) 1073 – 1082

Physics Procedia

8th International Conference on Photonic Technologies LANE 2014

NIR-CW-Laser Annealing of Room Temperature Sputtered ZnO:Al

V. Schütz[a,*], V. Sittinger[b], S. Götzendörfer[c] , C.C. Kalmbach[a], R. Fu[a], P. von Witzendorff[a], C. Britze[b], O. Suttmann[a], L. Overmeyer[a]

[a]*Laser Zentrum Hannover e.V., Hollerithallee 8, 30419 Hannover, Germany*
[b]*Fraunhofer IST, Bienroder Weg 54E, 38108 Braunschweig, Germany*
[c]*Berliner Glas Surface Technology, Giengener Strasse 16, 89428 Syrgenstein-Landshausen, Germany*

Abstract

Transparent Conducting Oxides (TCOs) are widespread as transparent electrodes in thin film photovoltaics and electronics. Post deposition furnace annealing improves the electrical and optical properties of TCOs. Disadvantages of furnace annealing are large energy consumption and long processing time due to long-lasting heating ramps. ZnO:Al thin films (AZO) with a low electrical resistivity and high transparency are usually sputtered at substrate temperatures up to several hundred °C. In this study post deposition near infrared (NIR) continuous wave (CW) laser annealing of room-temperature deposited AZO thin films is investigated. The surface temperature is determined by infrared thermography. The averaged transmittance is increased by $T_{300\text{-}1100\ nm} \leq 7.2$ % due to a lower absorptance at a constant reflectance. The resistivity is reduced to $\rho = 360$ µΩcm, because of a higher electron mobility μ. These promising results show the potential of laser annealing for the replacement of furnace annealing in industrial applications.

Peer-review under responsibility of the Bayerisches Laserzentrum GmbH

Keywords: Laser-Annealing; TCO; electro-optical parameters

* Corresponding author. Tel.: +49-(0)511-2788-329 ; fax: +49-(0)511-2788-100 .
E-mail address: v.schuetz@lzh.de

Peer-review under responsibility of the Bayerisches Laserzentrum GmbH
doi:10.1016/j.phpro.2014.08.020

1. Introduction

Transparent Conducting Oxides (TCOs) are widespread as transparent electrodes in thin film photovoltaics, electronics, and touch screen applications. Qualitative good thin film TCOs are characterized with a high optical transmittance at a simultaneous high electrical conductivity, resp. a low sheet resistance of the thin film. These requirements can be achieved with RF-magnetron sputtering, Kim et.al. (2010), Charpentier et.al. (2013) and Ruske et al. (2010).

Thin film DC-sputtering at room temperature yields in comparison to RF-sputtering a poor quality TCO. The opto-electrical properties of these TCOs can be enhanced with a thermal post process annealing in a furnace, Ruske et al. (2010). The thermal post process annealing time ranges in the regime of several hours, Wimmer et.al. (2012).

The processing time can be reduced via rapid thermal annealing, e.g. with uv-laser radiation. UV-laser radiation is absorbed by the TCO at the surface due to the short optical penetration depth d_{opt} in ZnO:Al. Therefore the surface is highly damaged, molten and reorganized after such a laser processing. The transmittance as a result is reduced. Such a ZnO:Al TCO applied on thin film µc-silicon solar cells has a worse external quantum efficiency, Johnson et.al. (2011). In contrast the transmittance of ZnO:Al in the near-infrared (NIR) wavelength range is high. Consequently, a homogenous thermo-optical annealing of the room temperature sputtered aluminum doped zinc oxides (RT-ZnO:Al) thin film could be achieved with near-infrared continuous-wave (NIR-CW) laser radiation.

For some applications scattering in the TCO-layer is desired. In thin-film photovoltaics, ZnO:Al is frequently used as a transparent front electrode. A short etching step in hydrochloric acid can give the ZnO:Al thin film a textured surface, Hüpkes et.al. (2012), which results in scattering of the transmitted light. This elongates the pathway of the photons through the cell and hence increases the probability of their absorption by the p-n-junction, thereby enhancing the efficiency of the cell, Dewald et.al. (2012). However, this “light trapping” effect can also be obtained by scattering induced by structured glass substrates, Ruske et.al. (2014). Similar textured glass is used in a wide field of applications, both for scattering in transmission (diffuse lighting, solar heat panels, and translucent windows) and in reflection (anti-glare surfaces for control panels, displays, etc.).

In this investigation RT-ZnO:Al is treated by laser radiation at different laser parameters, different ambient atmospheres on plane and structured glass substrates to enhance the initial optical transmittance and reduce the initial sheet resistance of the TCO. A much smaller laser annealing time of < 1 ms is sufficient to achieve opto-electric results which are comparable to furnace annealing at several hours, Ruske et.al. (2010). In contrast to UV laser annealing with melting and reconsolidation of the TCO no additional defects are induced by homogenous thermo-optical annealing with NIR-CW laser radiation due to solid state material changes.

2. Experimental details

2.1. Materials

In this laser annealing study on ZnO:Al different substrates and surface morphologies are investigated. The glass substrates are in general a low-iron soda-lime float glass from different suppliers (Berliner Glas “BG”, Euro Glas “EG”, Corning Glas “CG”) in order to investigate the general dependency of the surface morphology and the corresponding light scattering. Structured glass substrates for light scattering and in series solar cell efficiency increase have been obtained by wet-chemical etching from Berliner Glas. In a first step, the substrates are treated with an acidic fluoride solution, resulting in pyramid-shaped structural elements with a lateral size of 0.5 to 2 µm, which is considered to be the optimum for application in Si-based thin-film solar cells, Stiebig et.al. (2009). A second solution based on diluted hydrofluoric acid has been used to transform the basic surface texture into an irregular grid of overlapping calottes. Other substrates have a plane surface.

2.2. Thin layer deposition

$ZnO:Al_2O_3$ has been deposited using a ceramic target with 2 wt.% aluminium by DC-sputtering in the Leybold A700V in-line coater at Fraunhofer IST at room temperature. An extra white float glass (Euroglas Eurowhite) and Corning Eagle XG glass has been used as substrate. Because of the non-alkali free glass, an additional layer of

SiO_xN_y (~100 nm) between the float glass and the ZnO:Al has been deposited to avoid degradation of layer properties and possible delamination on the float glass samples. The deposited films have been measured with a Cary 5 UV-VIS-NIR spectrophotometer which provides a value of the layer thickness of d = 589 nm as the data has been fitted with an adequate model like Leng-Sernelius, Pflug et.al. (2004). The thickness has been additionally verified by a profile measuring system (Dektak).

Table 1. Deposition conditions for ZnO:Al films produced by DC magnetron sputtering.

Dynamical deposition by DC magnetron sputtering in the in-line facility Leybold A700V, PK 750 cathode		
Target substrate distance	d_{ST}	90 mm
Target material		$ZnO:Al_2O_3$ 2 wt.% Al /
Deposition pressure	p_{tot}	350 mPa
Argon flow	$q(Ar)$	199.8 sccm
Oxygen flow	$q(O_2)$	0.2 sccm
Substrate temperature	T_s	room temperature
Carrier velocity	v_c	0.6 mm/s
Excitation power	P	4.0 kW
Substrate		Corning Eagle XG, Eurowhite Float

2.3. Laser processing

The laser annealing setup consists of a cw fiber laser source (λ = 1070 nm, M^2 = 1.15), a galvanometric-scanner system to deflect the laser beam, and a process chamber for processing in different atmospheres, similar to Haupt et.al. (2011). The scanner is equipped with a dichroitic f-theta objective with a focal length of 255 mm. A laser focus diameter at the sample surface at $1/e^2$ $d_{foc} \approx 80$ µm has been measured using a Primes "MicroSpotMonitor©". Larger spot diameters of typically 550 µm are set by defocussing the laser beam. In this investigation all laser experimental conditions can be described with the two parameters laser intensity I as a function of the laser power P and the spot area A

$$I = P / A \tag{1}$$

and the laser-material interaction time t_{ww} as a function of spot diameter d_{spot} and the scribing velocity v_s

$$t_{ww} = \frac{d_{spot}}{v_s}. \tag{2}$$

2.4. Electrical, optical and thermal characterization

The electrical characterization is done by determining the sheet resistance R_{sq} via a four-point-probe measurement. The layer thickness dependent specific resistivity $\rho(d)$ is determined with

$$\rho = R_{sq} \cdot d \tag{3}$$

Further electrical parameters, like electron mobility μ_e are measured via Hall-Effect. The automatically detected error of the hall measurement is typically very small (around 10^{-4}-10^{-2} of the measured value) and therefore not given in data presentation, e.g. in Fig. 6 b.

The optical characterization is performed with a UV/VIS/NIR PerkinElmer spectrometer. The arithmetic mean of the optical parameters, e.g. T_m of the transmittance T is calculated in the wavelength range 300 nm ≤ T ≤ 1100 nm to have a compressed data presentation of the observed optical laser annealing results.

The thermal characterization is performed with the thermo camera Infratec "ImageIR8300©" via the temperature rise due to laser processing. The maximum temperature T_{max} at the surface due to certain laser parameters is used to associate laser parameters with the characteristic annealing temperature for comparison with literature.

3. Results and discussion

The TCO characteristics are changed by laser processing as a function of the applied laser parameters, TCO composition and surface structure. The initial partly small mechanical, optical and electrical layer differences modify the laser annealing process, so that in all cases the optimum laser parameters have to be identified individually.

3.1. Initial characteristics

The substrate morphology varies between a plane surface and a highly structured surface with a cup-form geometry. The different structured surfaces have been imaged by AFM, Fig. 1. A plane surface is shown from the top and the side. The thickness of the oxide layer can be distinguished by a brighter appearance in comparison to the glass substrate, Fig. 1.

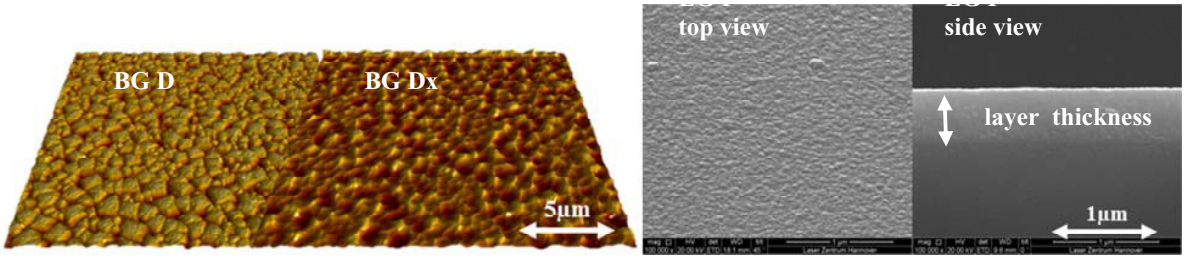

Fig. 1. Surface structures "D, Dx" chosen for laser annealing with an on top sputtered ZnO:Al; plane "P" surface shown for "EG"; AFM and SEM images.

The spectral transmittance T of the glass substrate is reduced by the TCO from approx. 95-96 % to approx. 75-80 %, Fig. 2 a. A typical wavy interference pattern for the transmittance T and reflectance R has been detected for plane substrates. In case of structured surfaces these wavy pattern are drastically smoothened and more homogenous patterns have been observed. In total the laser annealing of four different substrate materials is presented in this work; the reference transmittance T and mean transmittance T_m are shown in Fig. 2. For the "EG"-substrate different gases have been used to shield the ZnO:Al layer from the oxygen in normal atmosphere.

3.2. Thermographic investigations

TCOs are typically annealed in a furnace for several hours. The annealing temperature is set and controlled via a user interface of the furnace. In laser processing, it is usually not possible to control the laser induced material temperature on the surface directly. The temperature distribution evolves as a function of the used laser parameters (Intensity I and laser-material interaction time t_{ww}) in the material and can be measured at the surface with the used thermo camera, Fig. 3. The emission coefficient ε is determined in the investigated temperature range, resp. spectral range of 2.0 µm ≤ λ ≤ 5.7 µm with the aid of a specific oven lacquer with a known emissivity $\varepsilon = 0.98$. The emissivity coefficient ε of the used TCO ranges between $\varepsilon = 0.52$ for untreated material and $\varepsilon = 0.32$ at high interaction times, resp. temperatures.

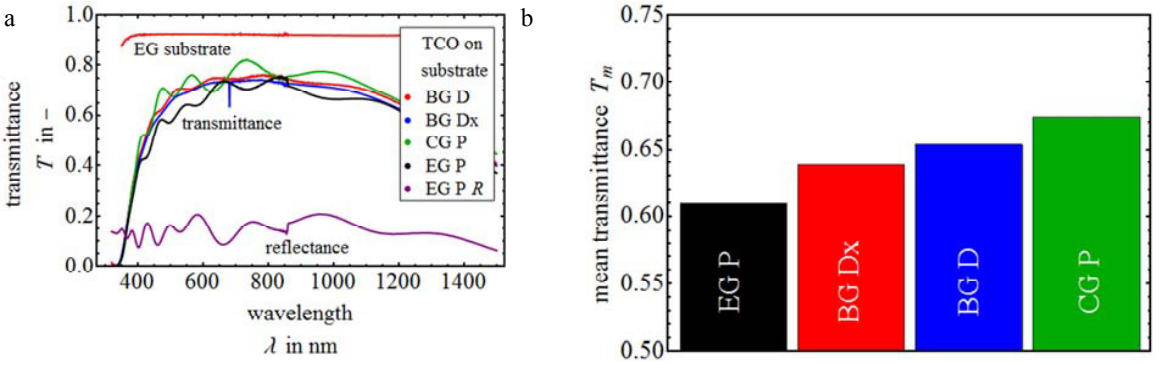

Fig. 2. (a) Exemplary spectral dependent transmittance T for plane and structured surfaces with exemplary reflectance R for plane "EG"; (b) Mean transmittance T_m for different substrates and surface structures; a ZnO:Al 2wt.% layer has been sputtered on top of all substrates.

The illustrated temperature ranges for different interaction times have been chosen due to the material and layer dependent process windows, Fig. 3b. The process window is defined where the TCO starts to delaminate and cracks appear in the glass substrate with high interaction times and where no annealing effect is observed at small interaction times. A similar maximum temperature at a much smaller annealing time is achieved with laser based rapid thermal annealing (RTA), compare with Kim et.al. (2005) and Charpentier et.al. (2013). Similar post annealing opto-electrical material properties have been determined for laser and furnace annealing, Chapter 3.3 and Charpentier et.al. (2013).

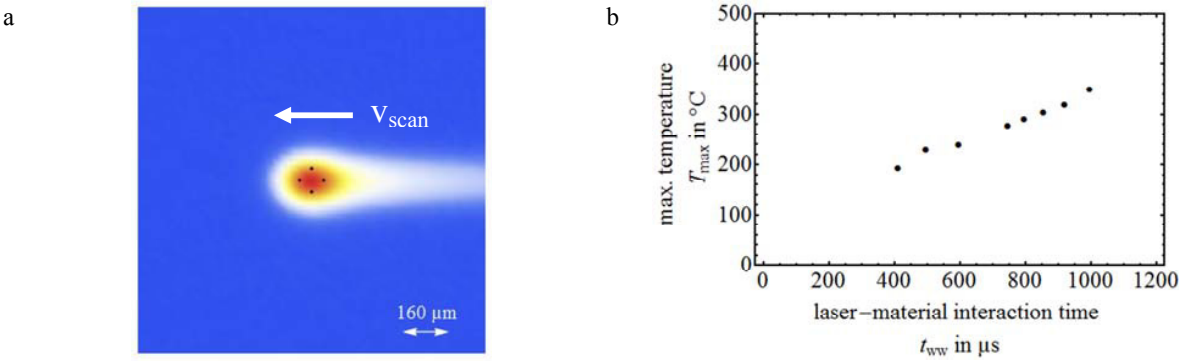

Fig. 3. (a) Thermography image of the laser annealing, black dots surround the maximum temperature T_{max}; (b) max. temperature T_{max} as a function of the laser-material interaction time t_{ww}, laser intensity I = 85.1 MW/m²; substrate "EG P".

3.3. Laser annealing

3.3.1. Fundamentals

Laser annealing can alter in analogy to furnace annealing the optical and electrical properties of room temperature DC-sputtered TCO ZnO:Al. Three characteristic optical material effects can be observed in all laser annealing experiments. The first one is characterized by the shift of the optical band gap E_g in the UV wavelength range due to an increased charge carrier concentration at the band gap, the so-called Burstein-Moss shift, Fig. 4 a. The shift is caused by heavy n-type doping in the conduction band. The second one is characterized by the shift of the plasma oscillation frequency w_p in the NIR wavelength range due to the same increase of the charge carrier concentration, Fig. 4 b. The measured free electron density has been initially around $N_e \approx 3 \cdot 10^{20}$ cm^{-3} and increases to approx. $N_e \approx 7.5 \cdot 10^{20}$ cm^{-3} at I = 106.4 MW/m^2 and t_{ww} = 912 µs. The third one is characterized by an increase of

the transmittance T in the VIS wavelength range, Fig. 4 c. A larger transmittance T is achieved with a better crystal quality which means a bigger grain size, a better orientation, and less crystal defects, Charpentier et.al. (2011) and Musat et.al. (2004). This explanation is also supported by the post laser annealing electrical material parameters, e.g. higher charge carrier concentration N_e and the higher electron mobility μ of the TCO, Fig. 6 c.

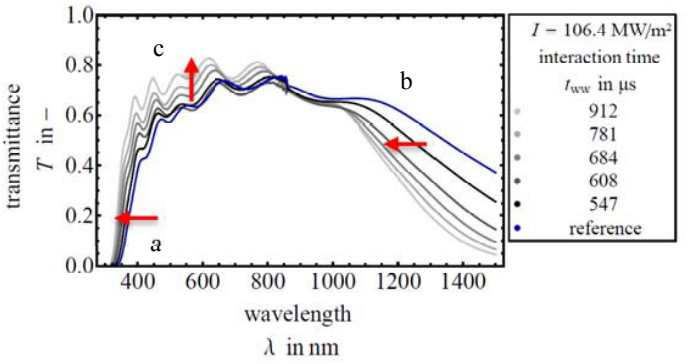

Fig. 4. Total spectral transmittance T as a function of the interaction time t_{ww} for substrate "EG"; laser annealing in atmosphere.

Further, a slight change of the surface morphology has been observed due to laser annealing. The surface gets smoothed by vanished nanostructures whereas the microstructures stay more or less unchanged, Fig. 5 a. Therefore, nearly no Haze H change (ratio between total and specular transmittance), with $H = (T_{total}\text{-}T_{specular})/T_{total}$, has been observed for $300 \leq \lambda \leq 1300$ nm, Fig. 5 b (black and gray curve).

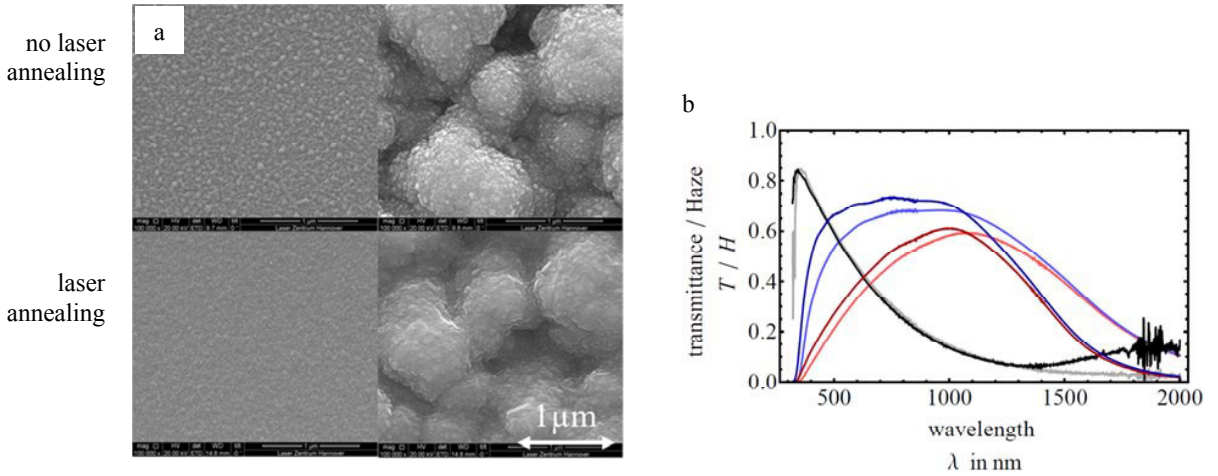

Fig. 5. (a) Morphological differences of ZnO:Al 2wt.% at the surface with and without laser annealing on a plane "EG "and structured glass substrate "BG"; SEM images; (b) spectral dependent specular (red colours), total (blue colours) transmittance and haze (black and gray colour), reference: lighter colours, laser annealing: darker colours (I = 85.1 MW/m² and t_{ww} = 912µs); substrate "BG".

Further, only the total transmittance T is considered in the following experiments description. The spectral reflectance R reveals to stay nearly unchanged in comparison to the reference over the whole spectral range.

3.3.2. Atmospheric conditions

The atmospheric boundary conditions influence the laser annealing of the ZnO:Al due to its specific content of oxygen in process atmosphere. The opto-electrical properties of ZnO can be altered with the Al dopant concentration and by doping with oxygen vacancies, Musat et.al. (2006). The laser annealing has been additionally

performed in two different inert gas atmospheres, Argon and Helium. As a second consequence, these gases have been chosen due to their different heat conductivities (one magnitude in difference) to investigate possible heat accumulation effects on laser annealing. For both inert gases different laser annealing parameters have been used to get a similar annealing result compared to processing in normal atmosphere. Although the peak value of the transmittance T is approximately the same to processing in normal atmosphere, the required laser-material interaction time t_{ww} for a successful annealing is reduced by a factor of 1/3 at the same laser intensity I, Fig. 6 a. An analogous behavior is observed for the electrical parameters, Fig. 6 b and c. The achieved minimal resistivity $\rho \approx 360$ µΩcm, Fig. 6 c with laser annealing is comparable to the ZnO:Al layers described in Szyszka et.al. (2012) with RF and DC-multipass deposition of ZnO:Al. As a result, the maximum transmittance T is not improved by the inert gases, but the processing time (interaction time t_{ww}) can be reduced for industrial applications. Further the reduction of oxygen in the laser processing atmosphere by inert gases enhances the possibility of doping ZnO with oxygen vacancies and in series the larger doping yields a reduced sheet resistance ρ. The difference in thermal conductivity of the inert gases has a minor effect on laser annealing of the used TCO. The observed small difference in Fig. 6 a (black and green curve) can also be explained with layer inhomogeneity.

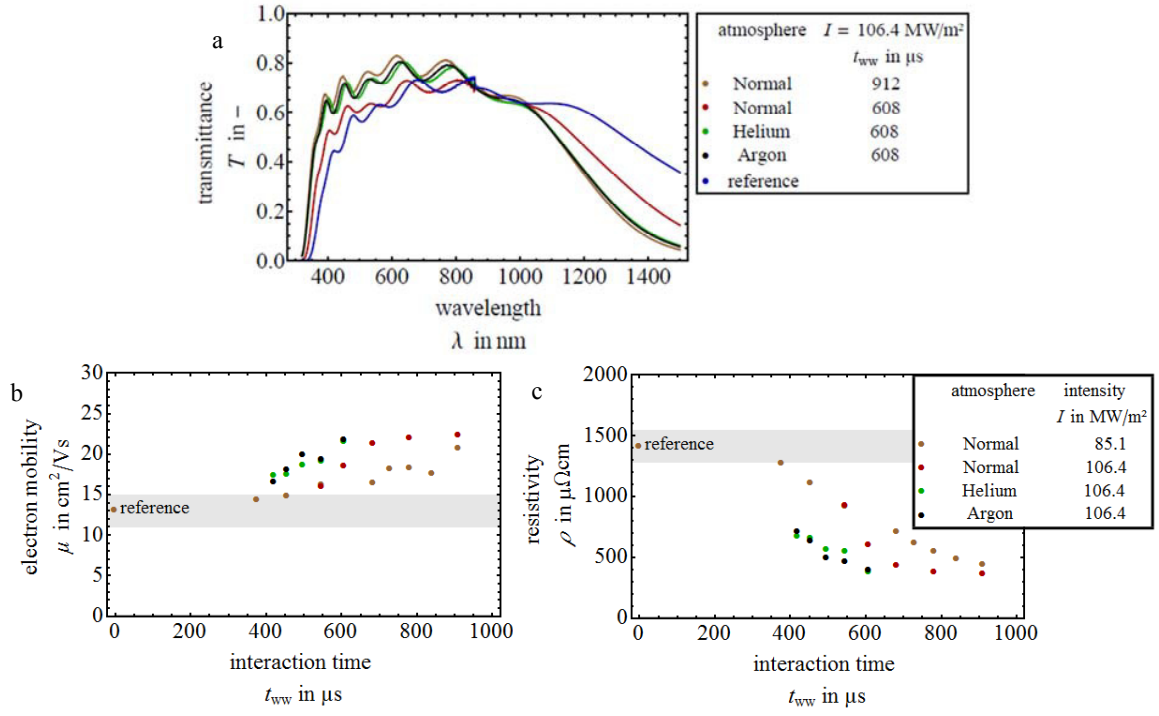

Fig. 6. (a) Spectral dependent transmittance T at different ambient conditions and two interaction times t_{ww}; (b and c) electron mobility μ and resistivity ρ as a function of the interaction time t_{ww}; substrate "EG P".

3.3.3. Substrate surface morphology

The substrate surface morphology influences the laser annealing of the RT-ZnO:Al due to its different layer growth and optical parameters, e.g. absorptance A. The crystal quality of ZnO:Al differs as a function of the substrate surface morphology. Well suited morphologies for ZnO:Al growth result in a large initial spectral transmittance, whereas in comparison worse suited surfaces have a smaller transmittance. Laser annealing of a compared worse grown RT-ZnO:Al on a substrate improves the crystal quality disproportionately high in comparison to a well grown TCO, compare in Fig. 7 "BG D" and "CG" to "BG Dx" and "EG". In series similar mean transmittances T_m have been determined after laser annealing, Fig. 7 b. The laser induced heat differs due to

the surface morphology dependent transmittance T, reflectance R and absorptance A. Although starting with initially different spectral transmittances T, laser annealing vanishes efficiently the mean optical differences due to different substrate surface morphologies and resulting transmittance T, compare Fig. 1, Fig. 5 a and Fig. 7 a. The smaller transmittance T increase can be explained by the laser induced heat load which is smaller for substrates with a larger transmittance T, resp. lower absorptance A at the used laser wavelength. This results finally in smaller annealing temperatures and a smaller improvement of the optical and electrical parameters of TCO.

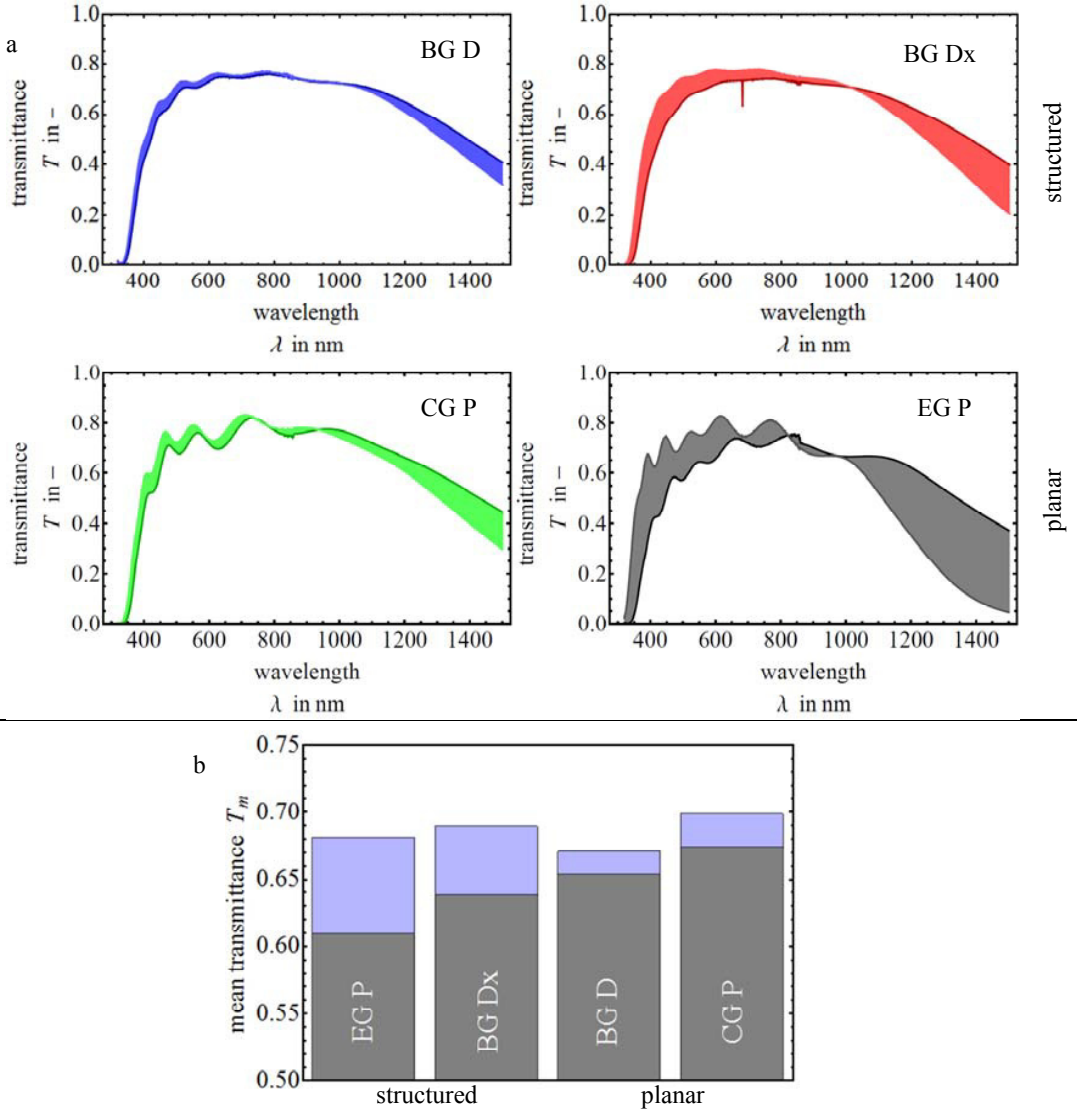

Fig. 7. (a) Spectral dependent transmittance T before and after laser processing for ZnO:Al 2wt.% sputtered on different substrates; the reference spectrum is visualized by darker lines, achieved spectrum by laser annealing with I = 106.4 MW/m² and t_{ww} = 912µs is shown with a filled area; (b) mean transmittance T_m before (gray) and after laser processing (violet).

The resistivity ρ decreases and the electron mobility μ of the ZnO:Al layer increases with rising interaction time t_{ww} consistently for all investigated substrates, Fig. 8. The absolute values differ by e.g. a maximum factor of 2.5 for the resistivity ρ, Fig. 8 b due to the different morphology specific heat loads applied by the same laser radiation

parameters. The determined laser parameter specific temperatures T_{max} in Fig. 3 b represent the achieved temperatures for the substrate "EG", whereas smaller annealing temperatures have to be considered for the other substrates, e.g. substrate "CG". Further, the substrates are differently suited for DC-sputtering of ZnO:Al. In the case of "BG D" worse initial electrical parameters are observed in comparison to the other investigated substrates, Fig. 8.

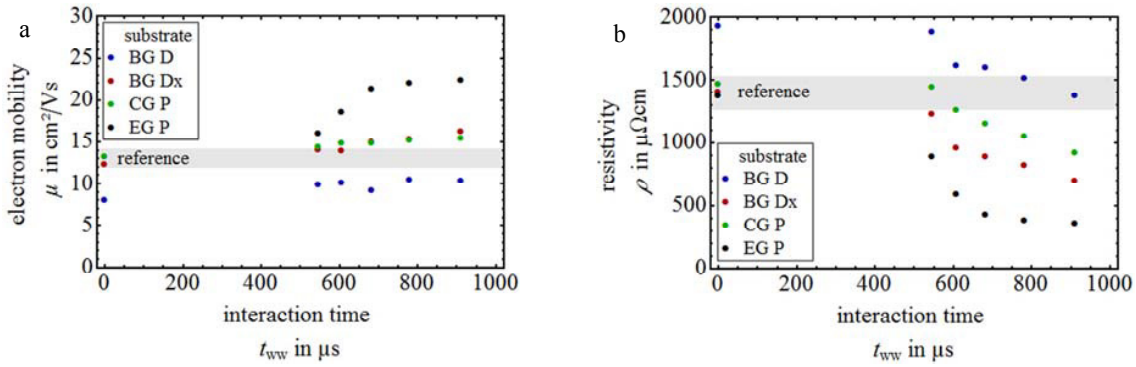

Fig. 8. (a) Electron mobility μ and (b) resistivity ρ as a function of the interaction time t_{ww} for different substrates; laser annealing in atmosphere; I = 106.4 MW/m².

4. Conclusions

The laser annealing with near-infrared continuous-wave (NIR-CW) laser radiation has been demonstrated for the room temperature DC-sputtered TCO ZnO:Al. The opto-electrical properties of this TCO are enhanced with this homogenous laser-thermo-optical annealing. The laser annealing for four different substrates and various process parameters, e.g. laser power has been investigated in terms of thermodynamic, optical and electrical parameters.

The thermodynamic laser annealing process window is determined by an upper process limit, where the TCO starts to delaminate and the substrate begins to crack. The lower process limit is characterized by a continuous transition to absent annealing with inappropriate laser parameters. Laser based rapid thermal annealing (RTA) yields a similar maximum temperature in comparison to furnace annealing at a much smaller annealing time. The annealing temperatures vary despite same laser parameters due to different surface morphologies and resulting transmittances. The heat conductivity of different inert gases (Argon and Helium) despite a difference of one magnitude does not significantly affect the laser annealing of ZnO:Al.

Three characteristic optical effects can be observed in all laser annealing experiments: (i) shift of the optical band gap E_g to larger photon energies, (ii) increase of the transmittance T in the VIS, (iii) shift of the plasma oscillation frequency w_p to larger photon energies due to a larger charge carrier concentration and an improvement of the ZnO-crystallinity without surface morphology change after laser annealing. In total a maximum arithmetic mean transmittance gain of ΔT = 7.2 % at a nearly constant mean reflectance R has been achieved.

The electrical parameters of the laser annealed ZnO:Al improve with larger laser intensities and laser-material interaction times. The resistivity decreases due to laser annealing at an increased charge carrier concentration and electron mobility, Table 2. The achieved electrical parameters for the room temperature sputtered ZnO:Al are comparable to ZnO:Al layer systems annealed by other methods or produced with different sputtering techniques but at much smaller annealing times.

Table 2. Achieved electrical parameters due to laser annealing.

parameter	initial	best
resistivity ρ in µΩcm	1400-1500	~360
charge carrier concentration N_e in 10^{20} cm^{-3}	~3	~7.5
electron mobility μ in cm^2/Vs	12-14	~23

The opto-electrical properties of ZnO can be altered by oxygen vacancies. The laser-material interaction time and in series the processing time is reduced by a factor of 1/3 using an Argon or Helium processing atmosphere for a comparable annealing to normal atmosphere due to the lack of oxygen during laser processing and possibly also in furnace annealing.

The laser induced heat load differs due to the surface morphology dependent transmittance T, reflectance R and absorptance A and influences the final annealing result optically and electrically.

Acknowledgements

This work has been funded by the German "Federal Ministry for the Environment, Nature Conservation, Building and Nuclear Safety", Contract No. 0325299A.

References

Kim, J.J., Lee, J.H., Bak, J.Y., et.al., 2010. Characteristics of low-temperature-annealed ZnO-TFTs. Journal of the Korean Physical Society 56-1, 404-408

Charpentier, C., Prod´homme, P., Roca i Cabarras, P., 2013. Microstructural, optical and electrical properties of annealed ZnO:Al thin films. Thin Solid Films 531, 424-429

Ruske, F., Roczen, M., Lee, K., et.al., 2010. Improved electrical transport in al-doped zinc oxide by thermal treatment. Journal of applied physics 107, 013708

Wimmer, M., Ruske, F., Scherf, S., et.al., 2012. Improving the electrical and optical properties of DC-sputtered ZnO:Al by thermal post deposition treatments. Thin Solid Films 520, 4203–4207

Johnson, E.V., Prod´homme, P., Boniface, C., et.al., 2011. Excimer laser annealing and chemical texturing of of ZnO:Al sputtered at room temperature for photovoltaic applications. Solar Energy Materials and Solar Cells 95-10, 2823-2830

Hüpkes, J., Owen, J.I., Pust, S.E., et.al., 2012. Chemical Etching of Zinc Oxide for Thin-Film Silicon Solar Cells. ChemPhysChem 13, 66-73

Dewald, W., Feser, C., Nowak, R., et.al., 2012. Light trapping in a-SI:H/µc-SI:H tandem solar cells on differently textured TCOS. Proc. 27th EU PVSEC, 2684-2688

Ruske, F., Schönau, S., Ring, S., et.al., 2014. Material properties of high-mobility TCOs and application to solar cells. Proc. SPIE 8998. Oxide-based Materials and Devices V, 898723

Stiebig, H., Haase, C., Schulte, M., et.al., 2009. Dünnfilm-Solarzellen mit strukturierten Oberflächen. Galvanotechnik 100-3, 646-652

Pflug, A., Sittinger, V., Ruske F., et.al., 2004. Optical characterization of aluminum-doped zinc oxide films by advanced dispersion theories. Thin Solid Films 455-456, 201-206

Haupt. O., Schütz, V., Stute, U., 2011. Multi-Spot Laser Processing of Crystalline Solar Cells. Laser-based micro-and nanopackaging and assembly V, 79210V

Kim, K.K., Tampo, H., Song, J.O., et.al., 2005. Effect of Rapid Thermal Annealing on Al Doped n-ZnO Films Grown by RF-Magnetron Sputtering. Japanese Journal of Applied Physics 44-7, 4776-4779

Charpentier, C., Prod´homme, P., Maurin, I., et.al., 2011. X-Ray diffraction and Raman spectroscopy for a better understanding of ZnO:Al growth process. EPJ Photovoltaics 2, 25002

Musat, V., Teixeira, B., Fortunato, E., et.al., 2004. Al-doped ZnO thin films by sol–gel method. Surface and Coatings technology 180-181, 659-662

Musat, V., Teixeira, B., Fortunato, E., et.al., 2006. Effect of post-heat treatment on the electrical and optical properties of ZnO:Al thin films. Thin Solid Films 502-1, 219-222

Szyszka, B., Dewald, W., Gurram, S. K., et.al., 2012. Recent developments in the field of transparent conductive oxide films for spectral selective coatings, electronics and photovoltaics. Current Applied Physics 12, S2-S11